Iğdır Üniversitesi Fen Bilimleri Enstitüsü Dergisi, 11(4): 2916-2925, 2021
Journal of the Institute of Science and Technology, 11(4): 2916-2925, 2021

ISSN: 2146-0574, eISSN: 2536-4618

Kimya / *Chemistry* **DOI: 10.21597/jist.912690**

Araştırma Makalesi / *Research Article*

Geliş tarihi / Received: 09.04.2021 **Kabul tarihi / Accepted: 16.08.2021**

To Cite: Arık M, Başar S.S, Demirci Gültekin D, Şen S, 2021. Bimolecular Interactions Between Graphene Oxide and a New Aza-BODIPY Derivative. Journal of the Institute of Science and Technology, 11(4): 2916-2925.

Bimolecular Interactions Between Graphene Oxide and a New Aza-BODIPY Derivative

Mustafa ARIK[1*], Serhat Salih BAŞAR[2], Demet DEMİRCİ GÜLTEKİN[3], Serkan ŞEN[4]

ABSTRACT: Fluorescent dyes are optical devices which are commonly used in medical and technical applications. Graphene-oxide, on the other hand, is a unique structure in nanotechnology with its oxygen-containing functional groups, high solubility, optical, electronic and thermal properties. Here we report photophysical properties of a newly synthesized fluorescent aza-BODIPY dye and dye-graphene oxide (GO) composite in aqueous media. Quantum yields were determined in both ethanol and chloroform medias according to Perker-Rees equation. Also quenching mechanism was discussed in the light of Stern-Volmer parameters.

Keywords: aza-BODIPY, graphene oxide, fluorescent, dye

[1] Mustafa ARIK (**Orcid ID:** 0000-0001-5788-4466), Siirt Üniversitesi, Sağlık Bilimleri Fakültesi, İş Sağlığı ve Güvenliği Bölümü, Siirt, Türkiye
[2] Serhat Salih BAŞAR (**Orcid ID:** 0000-0000-0000-0000), Erzurum İl Sağlık Müdürlüğü, Destek Hizmetleri Başkanlığı, İdari Hizmetler Birimi, Erzurum, Türkiye
[3] Demet DEMİRCİ GÜLTEKİN (**Orcid ID:** 0000-0003-0773-6048), Atatürk Üniversitesi, Aşkale Meslek Yüksek Okulu, Makine ve Metal Teknolojileri Bölümü, Metalurji Programı, Aşkale, Erzurum, Türkiye
[4] Serkan ŞEN (**Orcid ID:** 0000-0001-6361-7137), Ordu Üniversitesi, Fen Edebiyat Fakültesi, Kimya Bölümü, Ordu, Türkiye

***Sorumlu Yazar/Corresponding Author:** Mustafa ARIK, e-mail: mustafa.arik@siirt.edu.tr

Bu çalışma Salih Serhat BAŞAR'ın Yüksek Lisans tezinden üretilmiştir.

INTRODUCTION

Aza-BODIPY molecules are constructed as complexes of BF_2 with azadipyrromethene ligands (AzaBOronDIPYrromethene). Aza dyestuffs are considered as active fluorophores in the chemical sensor field. Recent studies point various applications such as laser dyes, sensors, photodynamic therapy, fluorescent probes, biological imaging, organic solar cells, and near-infrared (NIR) absorbing materials. Aza-BODIPY derivatives are excellent candidates for cancer therapy because of their low toxicities, NIR absorption and tumor-targeting abilities. They also offer pharmacokinetic desirable properties as photosensitizers (Chen et al., 2020). Aza-BODIPYs, which can also be designed with amphiphilic properties, can be dissolved in a wide range of solvents (Zuo et al.,2020). These molecules, which are known to be used frequently in sensor applications, have also been used in the determination of biogenic diamines with the advantage of their biocompatibility (Li et al., 2020). In recent decades, as the areas of use have increased, it has become more important to determine the photophysical properties of these compounds (Killoran et al., 2002). Because minor changes in the structure of aza-BODIPY compounds can significantly affect their fluorescence properties (Loudet and Burgess, 2007). Herein, a new aza-BODIPY dye containing fluorine (Figure 1), which has derivatives studied before has been synthesized to contribute the literature (Gorman et al., 2004; Hall et al., 2005; Ziessel et al., 2007; Lu et al., 2014). Synthesized dye 5,5-difluoro-1,3,7,9-tetrakis(4-(2-(2-(2-methoxyethoxy)ethoxy)ethoxy)phenyl)-5*H*-4λ^4,5λ^4-dipyrrolo[1,2-*c*:2′,1′-*f*[1,3,5,2]triazaborinine was named as Molecule 6 for a better understanding of synthesis steps.

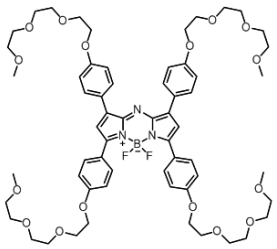

Figure 1. Chemical structure of Molecule 6

MATERIALS AND METHODS

Synthesis of Molecule 6

To synthesize Molecule 6, firstly triethyleneglycol monomethyl ether was reacted with p-TsCl in the presence of NEt_3 at room temperature and tosylate derivative **1** was obtained. For the purification of the compound, after washing with water, silica gel column chromatography (EtOAc) was used and 1 was obtained with 90 % yield. Afterwards, 1 was reacted with 4-hydroxyacetophenone and 4-hydroxybenzaldehyde, respectively, under the conditions of Williamson ether synthesis, and the corresponding 4-substituted derivatives **2** and **3** were obtained by purification by silica gel column chromatography (CH_2Cl_2) with yields of 90 % and 85 %, respectively. The unsaturated ketone derivative **4** obtained by condensation of these compounds in ethanol in the presence of 10 % NaOH was purified by silica gel column chromatography (EtOAc) in 80 % yield. By adding nitromethane to compound 4 under Michael addition reaction conditions, nitro ketone compound **5**, which is the precursor of the aza-BODIPY derivative, was obtained. Silica gel column chromatography was used for purification (EtOAc / MeOH: 99/1). (Yield: 85 %). The azadipyrin derivative obtained by heating the molecule **5** with ammonium acetate in n-butanol was reacted with $BF_3.OEt_2$ in dichloromethane in the presence of NEt_3 and dark navy blue Molecule 6 was synthesized. Silica gel column chromatography (EtOAc / MeOH: 97/3) was used for the purification of this compound and was

obtained in 60 % yield. The structure of Molecule 6 was determined by ^{1}H-NMR and ^{13}C- NMR spectroscopy techniques.

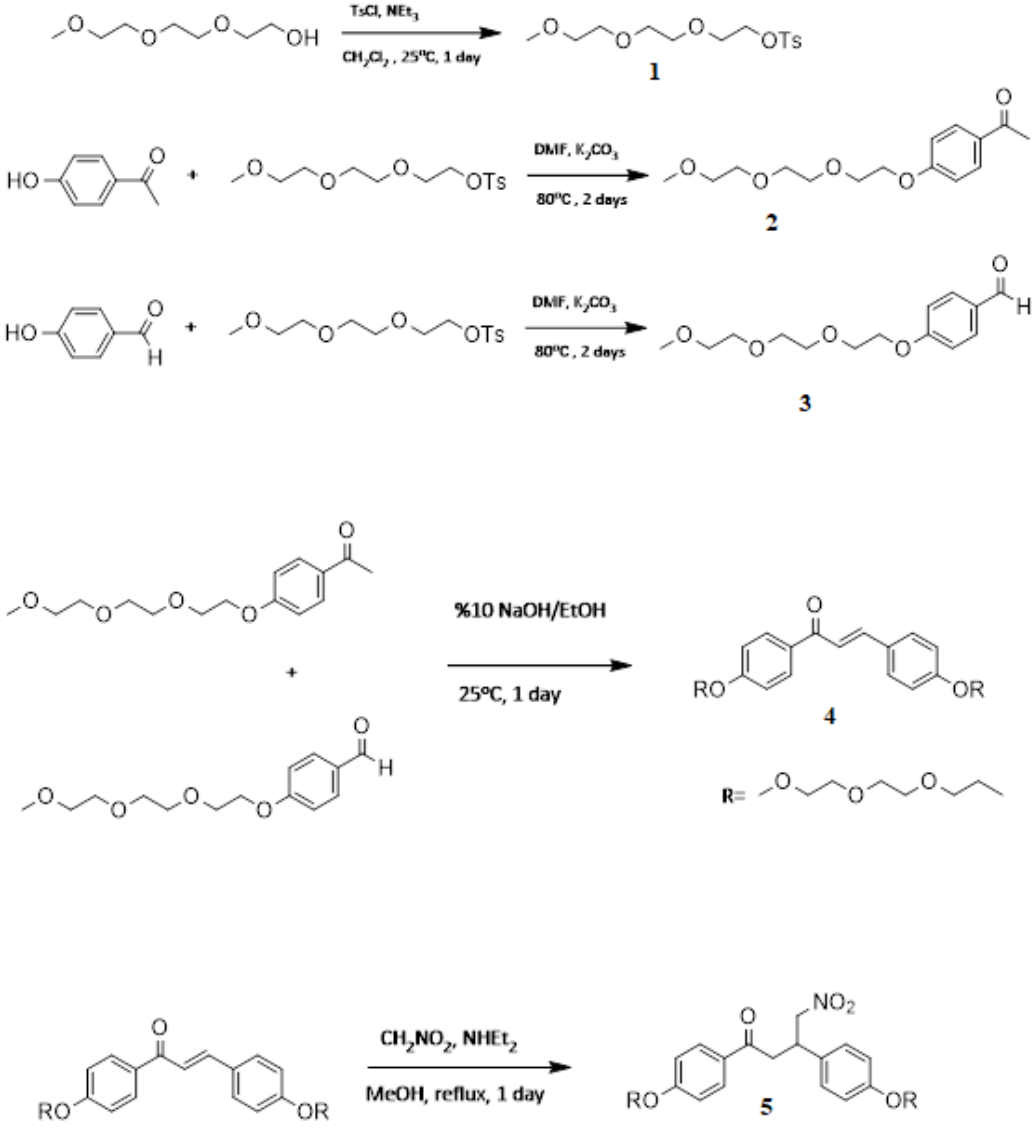

Figure 2. Synthesis of nitroketon compound **5**

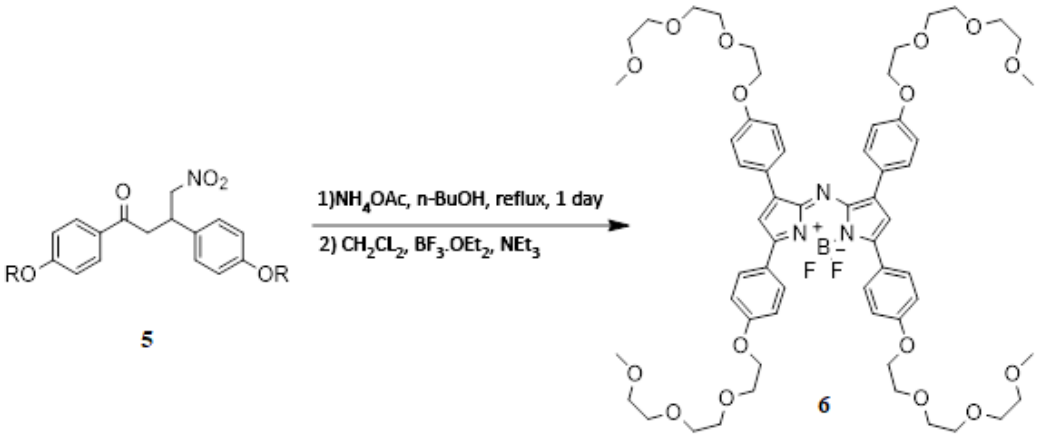

Figure 3. Synthesis of Molecule 6

Synthesis of Graphene Oxide

Graphene oxide (GO) preferred as quencher in this study is the oxidized form of graphene. Structurally, there are hydroxyl and epoxy groups on the main plane and carboxyl groups on the edges

(Dreyer et al., 2010). Graphene oxide is used in many areas such as supercapacitors (Zhang et al., 2012), solar cells (Narayanan et al., 2012), sensors (Balapanuru et al., 2010), electronic devices (Petersen et al., 2012), adsorption (Ramesha et al., 2011), Li- ion batteries (Zhu et al., 2011).

GO is obtained by reducing the number of layers of graphite oxide. Mostly Hummers or modified Hummers methods have been used for graphite oxide synthesis in the literature (Dimiev and Tour, 2014). For this purpose, 1 g graphite and 1 g $NaNO_3$ were mixed and dissolved in 50 mL 98 % H_2SO_4 and the system was cooled to 3 $^{\circ}$C in an ice bath. Then 6 g of $KMnO_4$ was added gradually and stirred in ice bath for half an hour. The temperature of the system was increased to 35 °C, and mixed for 3 hours. The mixture was transferred to an ice bath, 50 mL of distilled water was added dropwise and stirred for another half hour. Another 100 mL of water was added to the system and after 10 minutes, 6 mL of H_2O_2 (35 %) was added dropwise. The resulting mixture was filtered and washed several times with 50 mL of warm distilled water. The part remaining on the filter paper was dried at 80 °C and graphite oxide was obtained.

A concentration of 1.0 mg / mL in pure water was prepared by graphite oxide obtained and it was separated into layers in an ultrasonic water bath for a few hours. This process was repeated to seperate graphite oxide into layers thoroughly. Then the solution was left at room temperature for a certain period of time. During this time, the larger and water-insoluble graphene oxide layers precipitated by gravitational force. Then the precipitated graphene oxides were carefully removed from the solution and a graphene oxide dispersion with a concentration of 0.85 mg / mL was obtained. This stock dispersion was used to prepare composite solutions of different concentrations.

Experimental procedure

All reagents used were commercially available. UV/VIS Absorption and fluorescence spectra: Perkin Elmer Lambda 35 UV/VIS spectrophotometer and a Shimadzu RF-5301PC spectrofluorophotometer with quartz cuvettes, 1.0 cm optical path length, respectively. Fluorescence and absorption measurements of Molecule 6 -GO were performed at 10 °C to 50 °C in aqueous media to obtain Stern-Volmer graphics. For the steady-state fluorescence measurements, all the samples were excited at 640 nm, and fluorescence intensities were recorded between 630 and 800 nm. Fluorescence quantum yields (ϕ_f) for Molecule 6 were calculated by using the Parker_Rees equation given below. Where *D* is the integrated area under the corrected fluorescence spectrum and *n* is the refractive index of the solution. The subscripts *s* and *r* refer to the sample and the reference, respectively. In addition, OD_s and OD_r are the optical densities for the sample and the reference at the excitation wavelength, respectively. For the determination of relative quantum yield values, cresyl violet in methanol was used as the reference (ϕ_f =0.54) was used as reference (Bouwer, 2011).

$$\phi_s = \phi_r \left(\frac{D_s}{D_r}\right)\left(\frac{n_s^2}{n_r^2}\right)\left(\frac{1-10^{-OD_r}}{1-10^{-OD_s}}\right) \quad (1)$$

^{1}H-NMR and ^{13}C-NMR spectra were performed with Varian 400 and Bruker 400 instruments; in $CDCl_3$.

^{1}H NMR (400 MHz, $CDCl_3$, 298 K): δ (ppm) 8.04 – 7.98 (m, 8H), 7.00 – 6.96 (m, 8H), 6.92 (s, 2H), 4.22 – 4.17 (m, 8H), 3.91 – 3.85 (m, 8H), 3.77 – 3.62 (m, 24H), 3.55 – 3.51 (m, 8H), 3.36 (s, 12H),

^{13}C NMR (100 MHz, $CDCl_3$, 298 K): δ (ppm) 161.2, 160.2, 131.7 130.9, 125.7, 124.6, 114.9, 114.9, 72.1, 71.0, 70.9, 70.8, 69.9, 69.8, 67.7, 59.3

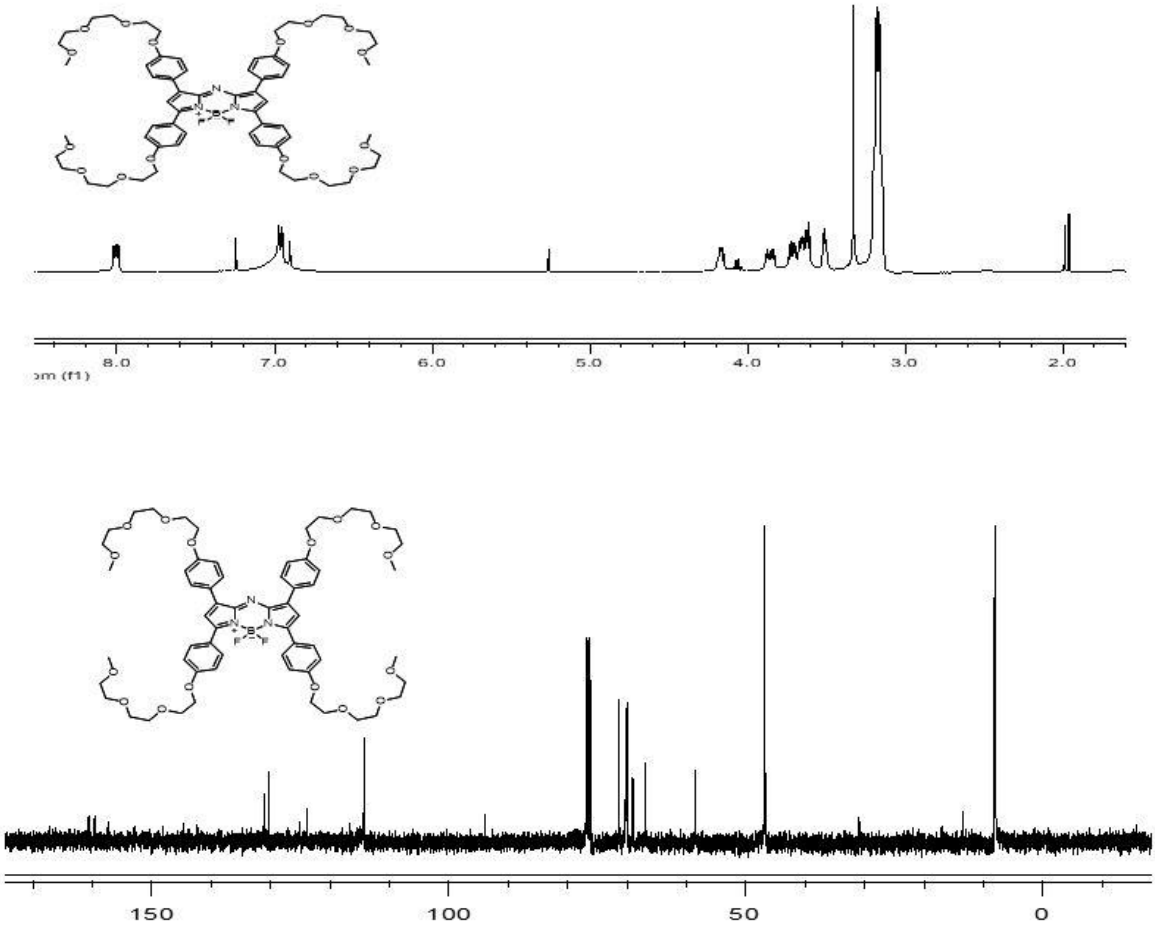

RESULTS AND DISCUSSION

Absorption and fluorescence spectra studies

The absorption and fluorescence spectra of the high purity Molecule 6 in chloroform (Fig 4a and 4b) and ethanol (Fig 5a and 5b) are parallel to the examples of azabodipy derivatives in the literature (Loudet and Burgess, 2007). When spectra are examined there is an increase in absorbance intensity with increasing concentration and the presence of a new band was not observed.

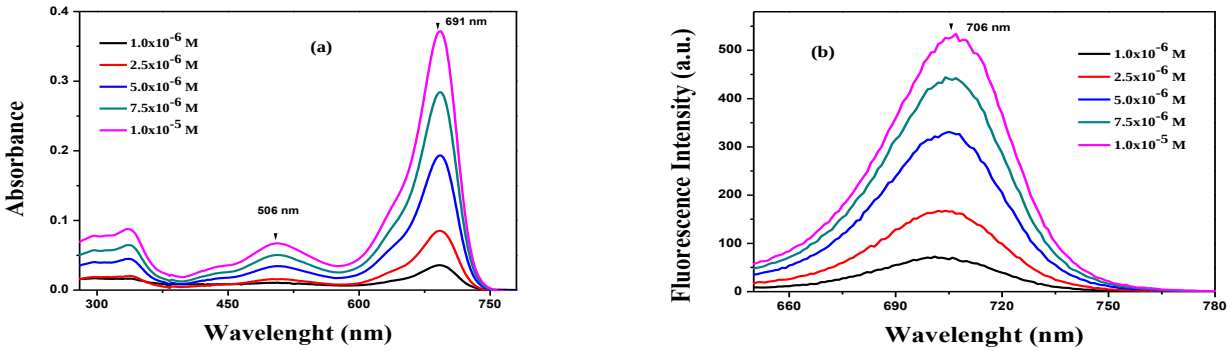

Figure 4. Absorption (a) and Fluorescence (b) spectra of aza dye in chloroform (λ_{exc}:640 nm)

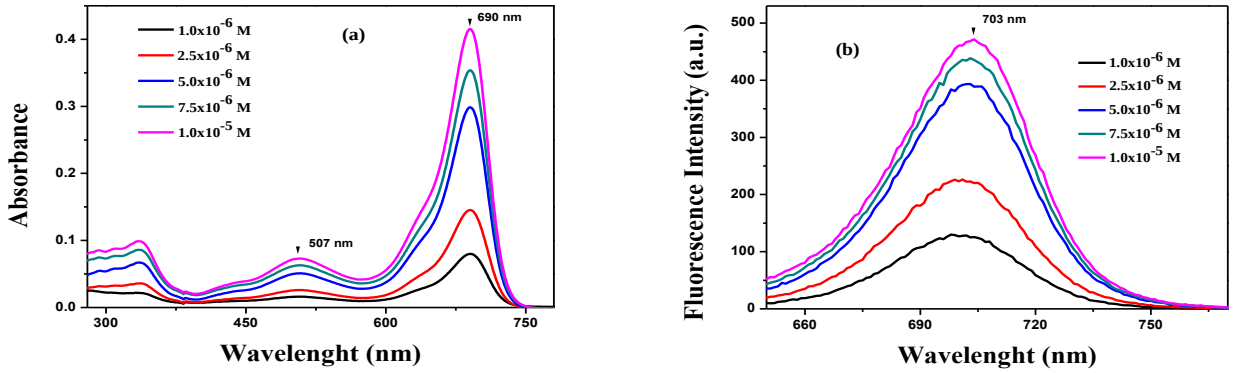

Figure 5. Absorption (a) and Fluorescence (b) spectra of aza dye in ethanol (λ_{exc}:640 nm)

Quantum Yields

The solution of cresyl violet (ϕ_f =0.54) in methanol was used as a reference in order to calculate the quantum yields. Figure 6 denotes the normalized absorption and emission spectra of cresyl violet in methanol. Quantum yields were calculated for aza compound in ethanol and chloroform media at different concentrations according to Parker-Rees method (Aydın et al., 2009). It was observed that quantum yields in chloroform (Table 1) were higher than quantum yields in ethanol.

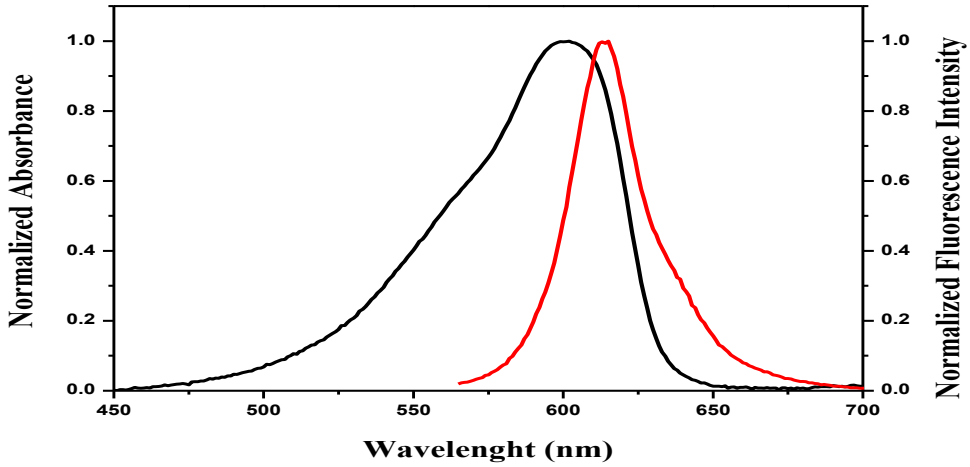

Figure 6. Normalized absorption and fluorescence spectra of cresyl violet in methanol

Table 1. Quantum yields for molecule 6 in ethanol and chloroform

Concentration	Chloroform	Ethanol
$1.0x10^{-6}$ M	0.115	0.094
$2.5x10^{-6}$ M	0.138	0.095
$5.0x10^{-6}$ M	0.125	0.087
$7.5x10^{-6}$ M	0.119	0.080
$1.0x10^{-5}$ M	0.112	0.075

Bimolecular Quenching Mechanisms

The interaction between two molecules is fundamental in the bimolecular quenching event. The collisions as a result of diffusion between molecules, and a photon absorption between molecules as a result of these collisions is defined as dynamic quenching. The formation of a non-fluorescent complex after the collision of fluorophore and quencher is known as static quenching. Quenching mechanisms are discussed with the Stern-Volmer equation (Lakowicz, 1983). Equations 1 and 2 are used to determine dynamic and static mechanisms, respectively.

$$I_o / I = 1 + Ksv[Q] = 1 + k_q \tau [Q] \quad (1)$$

$$I_o / I = (1 + Ksv[Q])(K_a[Q]) \quad (2)$$

In these equations, I_o is the fluorescence intensity when there is no quencher in the environment and I is the fluorescence intensity when quencher is present in the environment. k_q is the bimolecular dynamic quenching constant and τ is the fluorescence lifetime when there is no quencher. [Q] is the concentration of the quencher. *Ksv* is the dynamic Stern-Volmer rate constant and it is equal to the product of k_q and τ. K_a is the complex forming constant.

Ambient viscosity, temperature, fluorescence lifetime and absorption spectra are important parameters to determine the quenching mechanism. If the temperature of the media is increased in dynamic quenching, the Stern-Volmer constants increase depending on the diffusion coefficient. On the other hand, in static quenching, the stability of the complex decreases with the increase in temperature. As a result, a decrease in Stern-Volmer constants occurs. The change in the absorption spectra of fluorophore and quencher can also be considered in elucidating the quenching mechanism. When quencher is added to the medium at constant fluorophore concentration in static quenching, an increase in the absorption spectrum is observed due to the formation of a dark complex. Due to the fact that the diffusion of quencher to the fluorophore does not affect the excited states of the fluorophore, no change in the absorption spectrum is observed (Zhao et al., 2010; Lakowicz,1983).

In this study, when the absorption and fluorescence spectra obtained by keeping the concentration of Molecule 6 constant in aqueous medium and increasing the GO concentration are interpreted, it is seen that the emission intensity of Molecule 6 decreases at all temperatures (10 °C-50 °C). This decrease in spectra (Figure 7a and 7b) indicates an interaction between Molecule 6 and GO in aqueous environment. For the interpretation of this interaction, the data obtained according to equation 1 (Table 2) were used in drawing Stern-Volmer graphs.

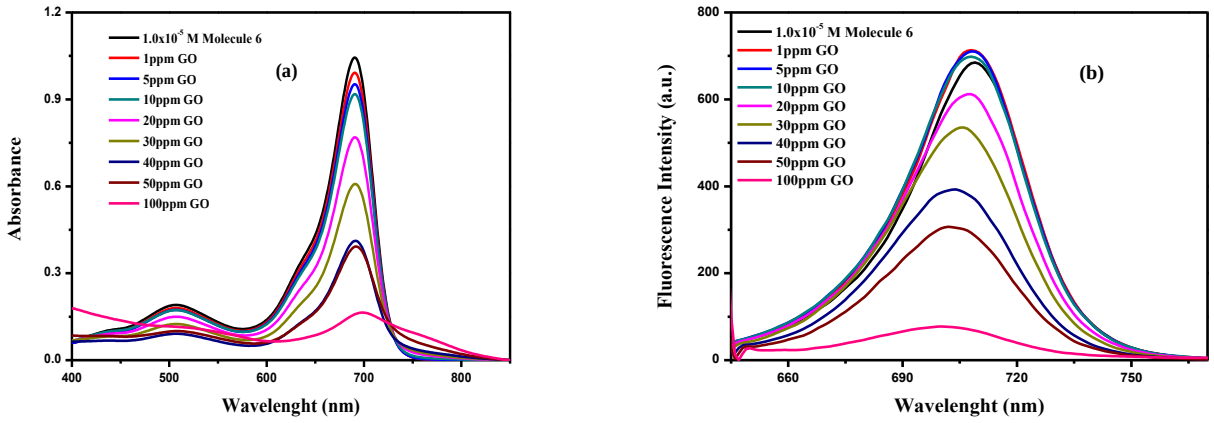

Figure 7. Absorption (a) and Fluorescence (b) spectra of GO added in increasing concentrations on $1.0x10^{-5}$ M solution of Molecule 6 at 20 ^{0}C (λ_{exc}:640 nm)

Table 2. Temperature dependent I_0/I values

	10 ºC	20 ºC	30 ºC	40 ºC	50 ºC
I_0/I	1.00 ± 0.05	1.00 ± 0.05	1.04 ± 0.05	1.03 ± 0.08	1.04 ± 0.07
I_0/I	1.07 ± 0.05	1.10 ± 0.06	1.63 ± 0.04	1.05 ± 0.04	1.10 ± 0.04
I_0/I	1.20 ± 0.05	1.20 ± 0.05	1.15 ± 0.07	1.13 ± 0.08	1.30 ± 0.09
I_0/I	1.41 ± 0.15	1.31 ± 0.10	1.41 ± 0.10	1.35 ± 0.09	1.40 ± 0.05
I_0/I	1.67 ± 0.11	1.58 ± 0.18	1.59 ± 0.20	1.57 ± 0.11	1.69 ± 0.22
I_0/I	1.99 ± 0.10	1.68 ± 0.10	1.83 ± 0.30	1.80 ± 0.20	1.86 ± 0.15
I_0/I	2.13 ± 0.14	1.91 ± 0.20	2.05 ± 0.10	2.03 ± 0.05	2.11 ± 0.10

When the Stern-Volmer graph drawn according to Table 2 is examined, the absence of a significant increase or decrease in the slope of the graph with the temperature increase indicates that the quenching is not static or dynamic alone (Figure 8).

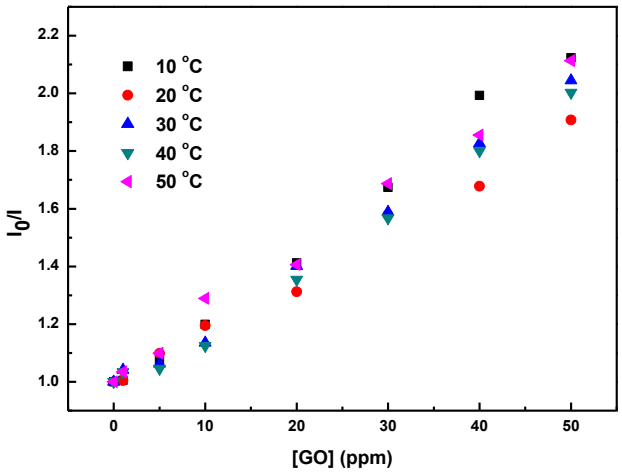

Figure 8. Change of Stern-Volmer graph with temperature for Molecule 6-GO interaction

According to this result, it is thought that static and dynamic quenching occur together as another possibility. For this purpose, it has been discussed whether the graphs drawn with the data in Table 2 are linear or not, taking into account equation 3. However, as seen in Figure 9, any linearity was not observed at any temperature.

$$\frac{I_0}{I} = (1 + K_D[Q])(1 + K_S[Q]) \quad (3)$$

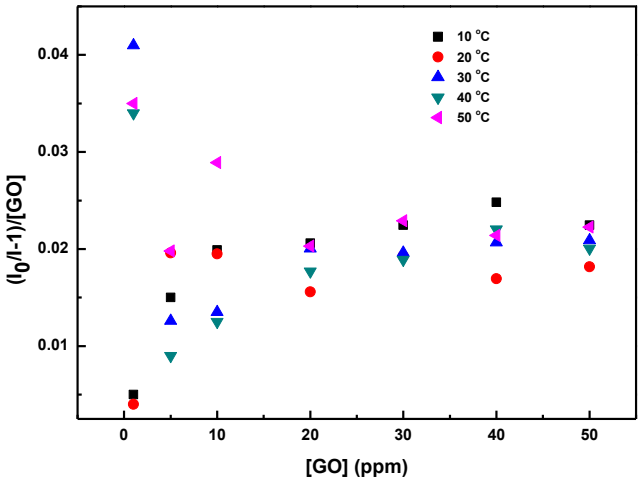

Figure 9. Quenching-linearity relationship of Molecule 6-GO

The calculations made according to equations 1-2-3 indicate that it is not possible to explain the quenching with stern- volmer parameters. Thus, it is thought that the decrease in fluorescence intensity in the Molecule 6 may be caused by the electrostatically adsorption of a part of this molecule on the surface of GO particles.

CONCLUSION

Herein, a new fluorescent aza-BODIPY derivative was synthesized and absorption and fluorescence spactra were recorded in ethanol and chloroform medias in different concentrations.

Fluorescent quantum yields were calculated according to Parker-Rees equation and found to be relatively low. Bimolecular interactions between the dye and graphene oxide were discussed taking in the account the quenching mechanisms. Studies conducted at different temperatures concluded that the decrease in fluorescence intensity of the dye molecule would only be due to electronic adsorption.

ACKNOWLEDGEMENTS

This study was supported by BAP Office of Atatürk University. Project no: FHD-2017-6181

Conflict of Interest

The authors declare no conflict of interest.

Author's Contributions

The authors declare that they have contributed equally to the article.

REFERENCES

Aydın BM, Acar M, Arık M, Onganer Y, 2009. The fluorescence resonance energy transfer between dye compounds in micellar media. Dyes and Pigments, 81:156-160.

Balapanuru J, Yang JX, Xiao S, Bao Q, Jahan M, Polavarapu L, Loh KP, 2010. A graphene oxide–organic dye ionic complex with dna-sensing and optical-limiting properties. Angewandte Chemie International Edition, 49(37):6549-6553.

Brouwer AM, 2011. Standards for photoluminescence quantum yield measurements in solution. Pure and Applied Chemistry, 83(12):2213-2228.

Chen D, Zhong Z, Ma Q, Shao J, Huang W, Dong X, 2020. Aza-BODIPY-Based nanomedicines in cancer phototheranostics. ACS Applied Materials & Interfaces, 12:26914-26925.

Dimiev AM, Tour JM, 2014. Mechanism of graphene oxide formation. ACS nano, 8(3):3060-3068.

Dreyer DR, Park S, Bielawski CW, Ruoff RS, 2010. The chemistry of graphene oxide. Chemical Society Reviews, 39(1):228-240.

Gorman A, Killoran J, O'Shea C, Kenna T, Gallagher WM, O'Shea DF, 2004. In vitro demonstration of the heavy-atom effect for photodynamictherapy. Journal of the American Chemical Society, 126(34):10619-10631.

Hall MJ, McDonnell SO, Killoran J, O'Shea DF, 2005. A modular synthesis of unsymmetrical tetraarylazadipyrromethenes. The Journal of Organic Chemistry, 70(14):5571-5578.

Killoran J, Allen L, Gallagher JF, Gallagher WM, Donal FO, 2002. Synthesis of BF2 chelates of tetraarylazadipyrromethenes and evidence for their photodynamic therapeutic behaviour. Chemical Communications, 17:1862-1863.

Lakowicz JR, 1983. Principles of Fluorescence Spectroscopy. Plenium Press, pp. 278-285, New York-USA

Li L, Li W, Wang L, Tang H, Cao D, Ran X, 2020. Pyrrolopyrrole *aza*-BODIPY dyes for ultrasensitive and highly selective biogenic diamine detection. Sensors & Actuators: B. Chemical 312, 127953:1-10.

Loudet A, Burgess K, 2007. Bodipy dyes and their derivatives: syntheses and spectroscopic properties. Chemical Reviews, 107(11):4891-4932.

Lu H, Mack J, Yang Y, Shen Z, 2014. Structural modification strategies for the rational design of red/NIR region bodipys. Chemical Society Reviews, 43(13):4778-4823.

Narayanan R, Deepa M, Srivastava AK, 2012. Nanoscale connectivity in a TiO2/CdSe quantum dots/functionalized graphene oxide nanosheets/Au nanoparticles composite for enhanced photoelectrochemical solar cell performance. Physical Chemistry Chemical Physics, 14(2):767-778.

Petersen S, Glyvradal M, Boggild P, Hu W, Feidenhans'l R, Laursen BW, 2012. Graphene oxide as a monoatomic blocking layer. ACS Nano, 6(9):8022-8029.

Ramesha GK, Kumara AV, Muralidhara HB, Sampath S, 2011. Graphene and graphene oxide as effective adsorbents toward anionic and cationic dyes. Journal of Colloid and Interface Science, 361(1):270-277.

Zhang LL, Zhao X, Stoller MD, Zhu Y, Ji H, Murali S, Ruoff RS, 2012. Highly conductive and porous activated reduced graphene oxide films for highpower supercapacitors. Nano Letters, 12(4):1806-1812.

Zhao Y, Li K, He Z, Zhang Y, Zhao Y, Zhang H, Miao Z, 2016. Investigation on fluorescence quenching mechanism of perylene diimide dyes by graphene oxide. Molecules, 21, (1642):1-7.

Zhu X, Zhu Y, Murali S, Stoller MD, Ruoff RS, 2011. Nanostructured reduced graphene oxide/Fe2O3 composite as a high-performance anode material for lithium ion batteries. ACS Nano, 5(4):3333-3338.

Ziessel R, Goze C, Ulrich G, 2007. Design and synthesis of alkyne-substituted boron in dipyrromethene frameworks. Synthesis, 06:936-949.

Zuo J, Pan H, Zhang Y, Chen Y, Wang H, Ren XK, Chen Z, 2020. Near-infrared fluorescent amphiphilic Aza-BODIPY dye: Synthesis, solvatochromic properties, and selective detection of Cu^{2+}. Dyes and Pigments, 183,108714:1-7.